Proceedings of PVP2007
2007 ASME Pressure Vessels and Piping Division Conference
July 22-26, 2007, San Antonio, Texas

PVP2007-26503

FLOW INDUCED PULSATIONS CAUSED BY CORRUGATED TUBES

Stefan P.C. Belfroid
TNO Science and Industry
Delft, The Netherlands
stefan.belfroid@tno.nl

Donald. P. Shatto
ExxonMobil
Houston, USA
Don.P.Shatto@exxonmobil.com

Rene M.C.A.M. Peters
TNO Science and Industry
Delft, The Netherlands
rene.peters@tno.nl

ABSTRACT

Corrugated tubes can produce a tonal noise when used for gas transport, for instance in the case of flexible risers. The whistling sound is generated by shear layer instability due to the boundary layer separation at each corrugation. This whistling is examined by investigating the frequency, amplitude and onset of the pulsations generated by 2" artificially corrugated tubes and cable feeds. Special attention is given to the influence of the geometry of the corrugations and to the influence of the boundary conditions of the tubes. Two distinct modes are measured. One high mode with a typical Strouhal number Sr=0.35 and one with a Strouhal number of Sr=0.1. The relative length scale for the corrugations to be used in the Strouhal number is a modified gap width, which is the gap width excluding the downstream edge radius. The exact Strouhal number for a corrugation is furthermore dependent on details of the corrugation, as the convective velocity of the flow disturbances is influenced by details in the geometry such as edge rounding. The amplitude of the generated pulsations scales with the acoustic pressure (ρcU) and will saturate for higher flow rates (p'/ρcU=constant). The saturation level is independent of pressure and tube length and is solely dependent on the corrugation geometry. Larger cavities will generate higher amplitude pulsations. The onset of the whistling is dependent on the tube itself and the system boundaries. Only for very long tubes is the onset insensitive to the system boundaries and will the onset be determined by corrugations. In that case the onset is determined by a critical boundary layer thickness. For smaller tubes, this critical layer thickness is still relevant, but the boundary conditions will have a large effect. A system with a high reflection coefficient will start at lower gas velocities than a system with a low reflection coefficient. Based on the current results the frequency and amplitude of the pulsations can be predicted.

INTRODUCTION

Corrugated tubes are used in many installations where flexible tubes are required. For instance flexible risers are used for the transport of gas from or to a platform. These risers have an internal corrugated profile (Figure 1). These corrugated tubes are prone to whistling, that is, the generation of pressure pulsations. For high pressure gas installations, the amplitude of these pulsations can be in the order of bars. Therefore, besides noise problems, integrity issues also arise due to the whistling.

Figure 1: Flexible riser inner carcass geometry.

The pulsations are generated due to vortex shedding and shear layer instabilities at the corrugations. At each corrugation a boundary layer grows which separates at the upstream edge of the corrugation. This forms an unstable shear layer which can dampen or magnify acoustic flow disturbances. If a coupling occurs with an acoustic field, for instance in the case of an acoustical resonance in the tube, a feedback mechanism occurs where the acoustical field is amplified by the shear layer instabilities and the acoustical field itself magnifies the layer instabilities.

The project focus was primarily experimental. Both field cases and laboratory experiments were used in the analysis. High pressure experiments (60 bar) were performed at the National Engineering Laboratory (NEL) with representative carcasses of 6-inch flexible pipes. At low and medium pressure conditions (TNO facilities and University of Eindhoven laboratory), experiments were done up to 12 bar with 2" commercial carcasses and a large number of tubes with artificially created corrugation. This allowed control of the corrugation geometry. In analyzing the behavior of the corrugated tubes, the interest was on the frequency and amplitude of the pulsations and on the onset of the generation of pulsations. Furthermore, the pressure drop across the corrugated tube and the passive acoustic behavior were measured and examined. The effects of the geometry of the corrugations, the tube length, and the boundary conditions were examined. In this paper the experiments with the artificial geometries and the cable feeds at low and medium pressure are discussed.

EXPERIMENTAL SETUP

The whistling behaviour of the corrugated tubes was examined by flowing air through them and measuring the upstream and downstream dynamic pressures. The use of multiple transducers allowed for reconstruction of the traveling and standing waves in these sections by using a multi-microphone method. The corrugated tube was set between two (1.605 m) long measurement sections, in which 2 sets of 5 transient pressure transducers were installed. With this setup, frequencies in the range of 31 to 2473 Hz could be reconstructed. By means of a back pressure control valve, the system could be pressurized to operational pressures up to 12 bar(a) (Figure 2).

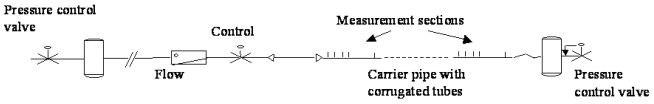

Figure 2: Experimental setup.

Besides the transient pressure transducers, the static pressure and temperature were measured in the downstream measurement section and the static pressure drop across the measurement section. The mass flow was measured upstream of the flow control valve. These data allow measurement of the flow velocities and the pressure drop across the corrugated tubes.

The downstream boundary condition was varied during the experiments. For most experiments a pressure vessel was used with a pressure control valve to control the operating pressure, but some experiments with direct outflow to the atmosphere have been performed. Finally, to evaluate the influence of the downstream boundary condition, the end of the measurement section could be terminated with an orifice. The open/pipe area ratio (a) of the orifice was varied from totally open a=1 to a=0.28, a=0.19 and a=0.1. Depending on the open area ratio the reflection coefficient could be changed at a given Mach number.

For corrugated tubes, both commercial tubes (carcasses of real risers and cable feeds) as well as artificial corrugated tubes (PVC) were used. In this paper the results using the artificial corrugated tubes and the cable feeds are presented. Artificial corrugations were used because they allowed for wide variation in edge radii, depths and widths of the corrugations. An overview of the variations tested in corrugation geometries is given in Table 1 with the geometry parameters defined in Figure 3. Besides symmetric corrugations also non-symmetric corrugations were made to test the influence of installation direction..

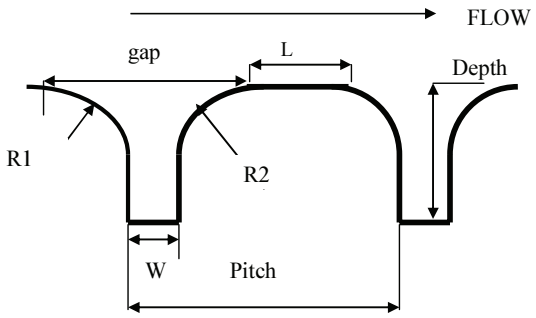

Figure 3: Definition of corrugation parameters.

Figure 4: Samples of artificial corrugated tubes.

A base experiment consisted of a velocity sweep starting at low velocity up to maximum allowed flow rates, which at atmospheric conditions was U=120 m/s. The total range of Reynolds numbers over which measurements could be made was from $Re=1\cdot10^4$ to $1\cdot10^6$. At different velocities (step size was approximately 0.4 m/s) a frequency spectrum was measured for each of the 10 pressure transducers. For those frequency peaks with a high coherence between the different measurement positions (per set of 5) a reconstruction was made based on the two-microphone method to reconstruct the upstream and downstream traveling waves. For each velocity this yields the upstream and downstream main frequencies, the amplitude of the pressure pulsations, and the pressure drop over the corrugated tube.

Table 1: Range of parameter variation

Geometry parameter	Variation
Tube Diameter [mm]	49 for artificial geometries 53, 65 for cable feeds
Pitch [mm]	8 – 16
Gap [mm]	4 – 12
L [mm]	0 – 8
W [mm]	2 – 8
R1 [mm]	0 – 4
R2 [mm]	0 – 4
Depth [mm]	2 – 7
Tube length [m]	≈3 for artificial geometries Up to 50 m for cable feeds

RESULTS

Frequency

At low velocity, below onset, no whistling behaviour is observed (Figure 5). Only the normal flow noise is measured with some acoustical resonances. At a given velocity the whistling starts and a clear tonal noise is generated. In this case only one tone was measured, but in general also harmonics are measured. At high velocities the frequency peak widens and contains multiple peaks. This is dependent on the spectral density of the corrugated tube and on the velocity difference upstream and downstream of the tube. A high spectral density allows for multiple peaks and for very large velocity differences, due to the pressure drop, multiple frequencies can be excited.

As function of the velocity, the corrugated tube generates tones at a specific Strouhal number. That is, the frequency increases linearly with increasing velocity (Figure 6). If the possible axial resonance modes are far apart in frequency, the generated tones can lock in at the distinct resonance frequencies, which result in a more stepwise change in frequency with increasing velocity.

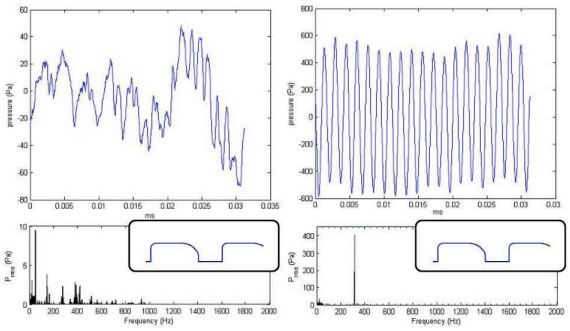

Figure 5: Time signal and frequency spectrum before (left) and after (onset). The geometry measured is given as insert.

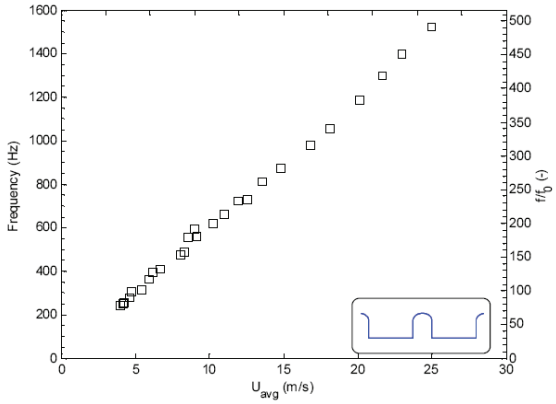

Figure 6: Frequency as function of (average) velocity. f_0 Is the first axial resonance frequency of the measurement setup.

It is customary to express the frequency as a Strouhal number (*Sr*) defined by :

$$Sr = \frac{fL}{U} \qquad (1)$$

with *f* the frequency [Hz], *U* the mean gas velocity in the tube [m/s] and *L* a characteristic dimension [m]. It is important to identify the correct length scale. For cavity flow and side branches this is the width of the cavity. For corrugated tubes it has been thought that the pitch would be the determining length scale. We considered three definitions for the length scale: the pitch, the gap width and a modified gap width (R1+W). This alternative definition is based on the findings of Bruggeman [2], [3] where for side branches with rounded edges it was found that the downstream edge radius did not play a role. In Table 2, for a selection of configurations the Strouhal numbers are given. It is clear that the pitch is not the correct length scale, as the two geometries 1 and 2 have a similar pitch but a very different Strouhal number. The differences for the definition of the gap or the modified gap are less clear. For the complete dataset the modified gap showed a slightly better collapse of the Strouhal numbers.

Table 2: Strouhal number for selection of configurations. R_{up} is the upstream edge radius.

pitch [mm]	gap [mm]	Rup+W [mm]	Sr_pitch [-]	Sr_gap [-]	Sr_Rup+w [-]
12	8	6	0.71	0.47	0.35
12	12	10	0.51	0.51	0.43
8	8	6	0.50	0.50	0.38

However, the Strouhal number is not uniquely defined by the adapted gap width. Still a large range of Strouhal numbers are measured. Furthermore, two sets of Strouhal numbers are measured. One 'high' Strouhal number around 0.23- 0.51 and one 'low' ranging from 0.04 to 0.2. These two Strouhal numbers form two modes. This is clearly seen in Figure 7, in which the Strouhal number is plotted as function of the dimensionless

corrugation volume. This is defined as the ratio of the corrugation volume to the volume of the corrugation and the inner pipe. For relatively large cavities, the Strouhal number is high. For small corrugations the Strouhal number is low. The mechanisms behind the different modes are not yet fully understood. The higher modes are thought to be associated with flow disturbances due to pressure disturbances. The lower mode is thought to be associated with vortex shedding initiated by acoustic velocity fluctuations. The first is the main mechanism for flow excitation in shallow cavities, while the last is the mechanism encountered in vortex shedding at for instance T-joints [2], [4].

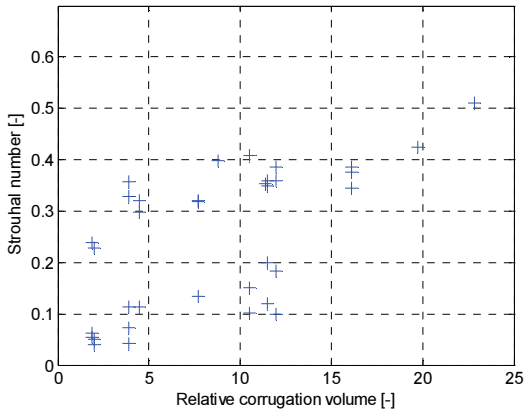

Figure 7: Strouhal number Sr_{Rup+W} as function of relative corrugation volume.

The reason for the dependence on the cavity geometry is the effective convective velocity of the disturbances in the cavity. For larger corrugations, which often means wider cavities, the disturbances enter the cavity more deeply and therefore, the effective velocity decreases. Of course, the details of the flow behaviour, such as the point of flow separation and streamline paths, are very dependent on the exact geometry of the corrugation such as the edge rounding.

An alternative relation between corrugation geometry and Strouhal number is found starting from the classical formulation for cavity flow according to Rossiter. This formulation gives the Strouhal number as:

$$\frac{fL}{U} = \frac{m - \xi}{M + 1/k_v} \qquad (2)$$

with $k_v = U_c / U$ the ratio of the shear layer velocity and the free-stream velocity, ξ an empirical constant, m the mode number, M the Mach number and L the cavity length. Standard values of k_v=0.57 and ξ=0.25 are generally used. This would lead to Sr_{gap}≈0.41. However, as was hypothesized in the previous section, the convective velocity is a function of the geometry. In Figure 8 the k_v parameter is plotted as function of the ratio of the upstream edge radius to the gap width. The high Strouhal mode corresponds to values for k_v≈0.6. For the lower Strouhal mode the values are between 0.1 and 0.2. For small edge radii the k_v value required to match the measured frequency is approximately k_v=0.85 which means that the disturbances almost convect with the main stream velocity. This value is higher than found in literature for cavity flow. For geometries with relatively large edge radii the required k_v value is approximately 0.5 which is more in line with the classical values.

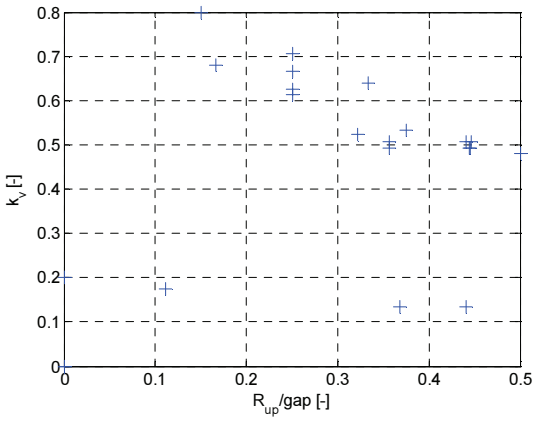

Figure 8: k_v parameter as function of the ratio of the upstream edge radius (R_{up}) to the gap width.

As confirmation, a limited number of numerical simulations were performed to calculate the velocity in the corrugation at a streamline leaving at the upstream edge rounding. In Figure 9 the numerical results are plotted as function of the same R_{up}/gap. The correlation between the experimental k_v and the numerical results are very good. More accurate simulations will be performed at a later stage.

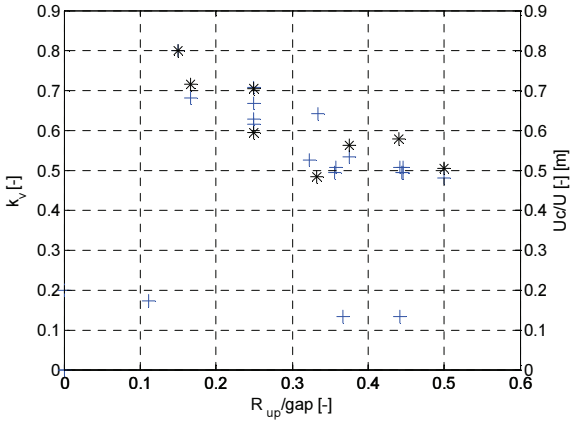

Figure 9: k_v parameter (crosses) and numerical results Uc/Umain (stars) as function of the ratio of the upstream edge ratius ((R_{up}) to the gap width. The numerical results are scaled to match one geometry (R_{up}/gap=0.25).

The Rossiter equation predicts a decrease in the Strouhal number as a function of Mach number. For most of the configurations this was also observed in the experiments. In Figure 10 the Strouhal number is plotted as a function of Mach number for one geometry in which this trend is observed.

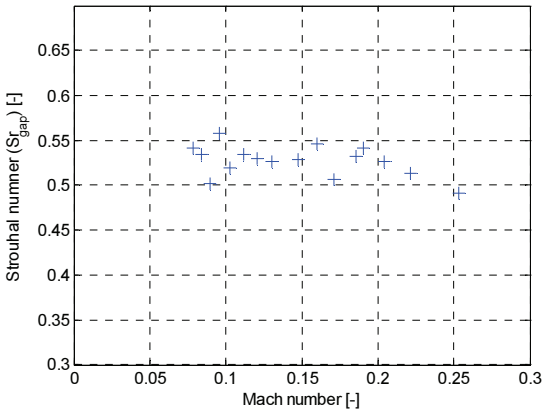

Figure 10: Strouhal number Sr_{gap} as function of Mach number.

Amplitude

The amplitude of the pulsations increases linearly with increasing velocity and operating pressure. In Figure 11 the measured amplitude is plotted as function of the velocity for different operating pressures. After onset the amplitude increases with increasing velocity whereafter a plateau is reached. Initially, it can occur that after onset the whistling behaviour disappears with increasing velocity. This probably is caused by the fact that reflections have decreased and therefore the energy containment in the tube for those conditions. With increasing velocity the whistling then often starts again.

The same pressure saturation level is reached independent of operating pressure or tube length (Figure 11 and Figure 12). This is important as this means that the phenomenon is a localized mechanism in which local saturation occurs. The saturation level is dependent on the corrugation geometry in which the volume of the cavities seems predominant. In Figure 13 the saturation level is plotted as function of the relative corrugation volume. It is clear that large cavities can generate higher amplitude pulsations than small cavities. A similar behaviour is observed by Anthoine [5].

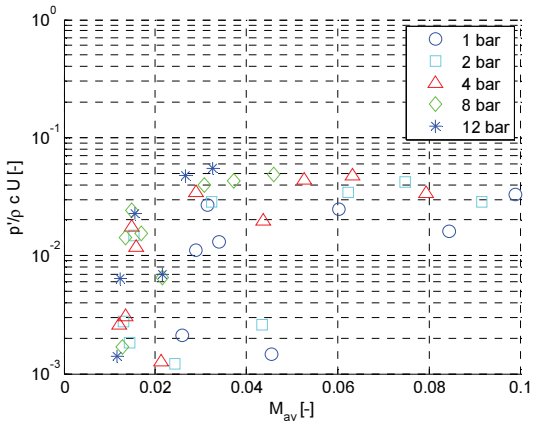

Figure 11: Dimensionless amplitude (average of upstream and downstream) as function of (average) velocity for different operating pressures.

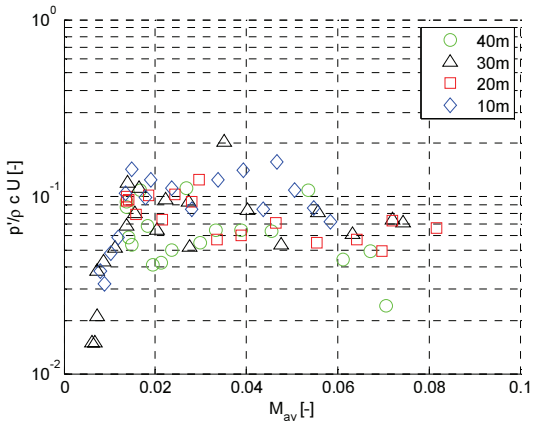

Figure 12: Pulsation amplitude as function of velocity for different tube lengths.

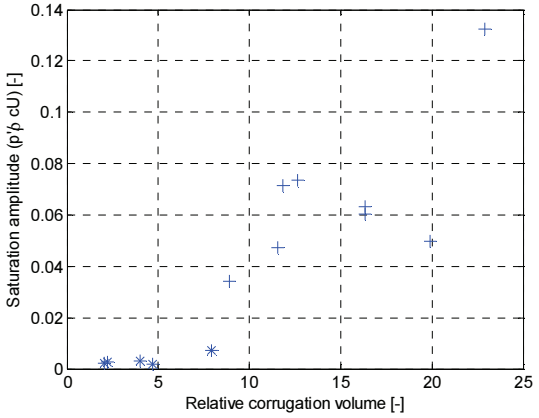

Figure 13: Saturation amplitude as function of corrugation volume. Crosses indicate full saturation level. Stars indicate geometries which did not fully reach saturation for maximum velocity.

Onset velocity

The onset velocity of whistling is very important for practical concerns. Corrugated tubes with a low onset velocity may limit the production capacity drastically. In determining the onset both the corrugated tube and the system in which the tube is installed are important. As discussed, the whistling behaviour is a feedback mechanism between the acoustic waves and instability of the shear layer. The system determines the energy fed back to the corrugated tube. This could mean that a positive feedback is required on both tube ends to start the whistling behaviour. For tubes with pronounced corrugations and small tube lengths the possible resonance frequencies in the tube determine the onset velocity. When the resonance frequency coincides with the excitation frequency onset will occur. However, lengths from several 100's of meters to several kilometers are used in commercial applications. The resonance frequency bandwidth for those tubes is very small, and the onset velocity is determined by other parameters, such as the corrugation geometry and the reflection coefficients at the ends of the tube. To investigate the boundary effect, the system boundaries were varied by using a multihole orifice as the downstream boundary condition. By changing the number of holes the effective open area ratio could be varied. This allowed for a variation in the downstream reflection coefficient. In total three different open area ratios (a) for the orifices are used (a=0.28, a=0.19 and a=0.1). Using the different orifices the reflection coefficient could be reduced to approximately |R|=0.2. This means that only approximately 5% of the energy is fed back to the corrugated tube.

Experiments have been done with a bellows type corrugated tube with very pronounced corrugations. Furthermore, different tube lengths have been used, ranging from 50m to 3m. This corresponds to length/diameter ratios from 45 tube diameters to over 770 diameters. In Figure 14 the dimensionless amplitude is plotted as function of the average Mach number (average of upstream and downstream Mach number) for the different orifice cases for the tube lengths of 50m, 10m and 3m. For the case of the 50m tube there is no effect of the downstream boundary condition. There is no effect on the onset velocity or on the pulsation amplitude. This is clear in Figure 15 where the pulsation amplitude is plotted as a function of the reflection coefficient. The limited effect is not true for the 10m case. Although, as 10m is still more than 150 tube diameters and constitutes nearly 6 wavelength at the onset at open end conditions, initially this was thought to be a long tube. However, with the orifices the onset is postponed to nearly double the onset velocity at open end conditions. This onset has not changed yet in comparison with the 50m case. When the tube length was even further decreased to 3m, which means 46 tube diameter and 1.75 wavelengths at onset frequency at open end conditions, the onset increased to double the value. The spread in onset velocity has even increased to a factor three.

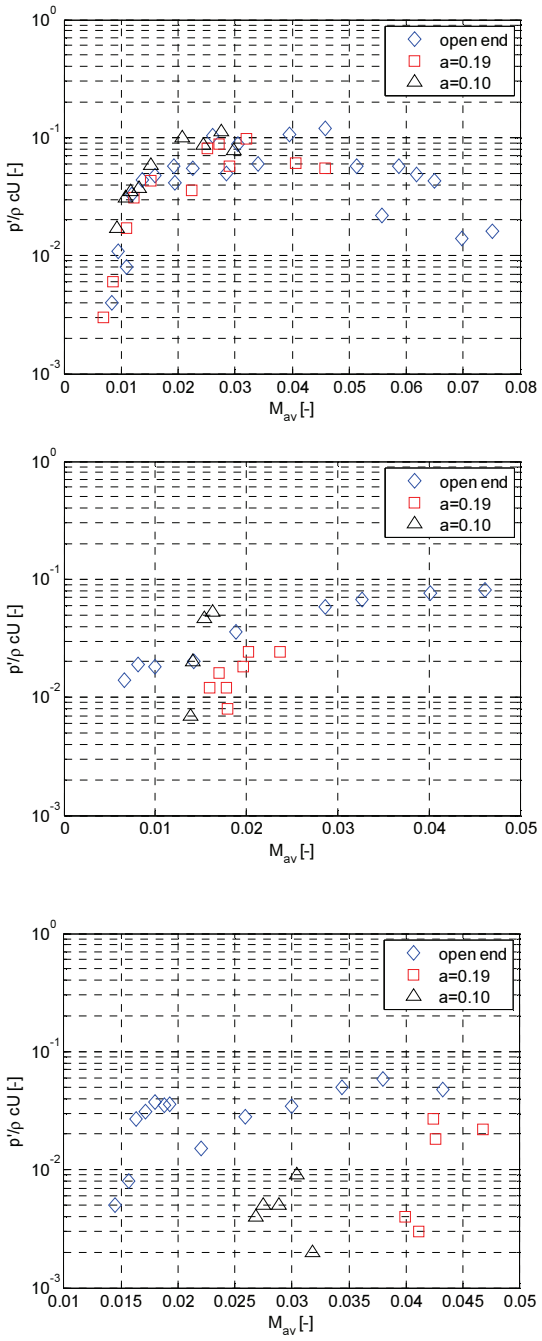

Figure 14: Dimensionless amplitude as function of (average) Mach number for different orifice open area ratios for a tube length of 50m (top), 10 m(middle) and 3 m (bottom).

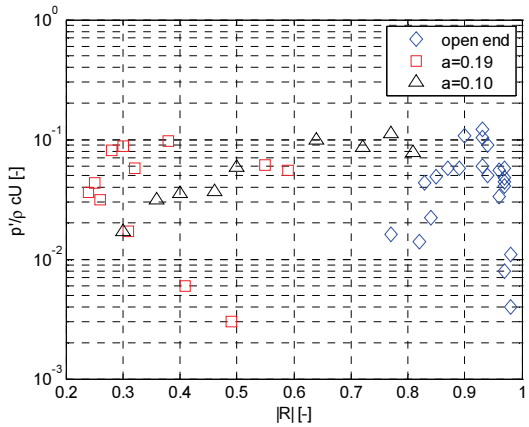

Figure 15: Dimensionless amplitude as function of reflection coefficient for different open area ratios with a tube length of 50m.

The influence of the boundary condition for the shortest tubes could be attributed to, for instance, the limited number of acoustic wavelengths present in the tube at a possible resonance or to entry length effects. It will take several tube diameters to get a new stable flow. The observation that for the long tube of 50m there is hardly effect of the downstream boundary condition would indicate that no resonances are necessary for very long tubes. This means that the self excitation is very strong and only a minimal energy feedback is required. However, as the boundary conditions also were important for the 10m tube, this conclusion is limited only to long tubes. A criterion has not yet been established. In a next phase of the project, the boundary effect will be investigated in more detail by extending the variation in boundary conditions.

Besides the boundary conditions, the corrugation geometry is, of course, a factor in the onset velocity. The whistling behaviour starts when a positive feedback occurs between the acoustical field and the unstable shear layer. From experiments on cavities and on side branches [2][7][8] it was concluded that there was a critical shear layer (momentum) thickness (in comparison to the cavity or branch width) above which the layer could not become unstable. With increasing velocity the shear layer becomes thinner and can become unstable. The same holds for the corrugations. In Figure 16 the measured onset velocity is compared to the theoretical onset velocity based on a critical boundary layer thickness. In general the measured onset velocities are higher than the predicted ones. This is due to the influence of the boundary conditions as discussed previously. Furthermore, there is uncertainty in predicting the boundary layer formation, as the exact start of the boundary layer growth and the separation point are unknown. The critical number (c_{crit}) used in Figure 16 is based on a match to one geometry. The best match to measured data was obtained assuming a laminar, flat plate boundary layer growth over the plateau, with the boundary layer growth starting partially on the downstream edge:

$$\frac{\theta}{gap} = c_{crit} = \frac{c_1 a\sqrt{\nu x/U}}{W} \qquad (3)$$

with c_1 the ratio of momentum thickness to boundary layer thickness ($c_1 \approx 0.13$), a the growth coefficient (a=5), ν the gas viscosity [m^2/s] and x the growth length. As said the best fit was obtained with the boundary layer growth starting partially on the downstream edge ($R_{downstream}$):

$$x = \tfrac{1}{2}\pi\left(a_1 R_{upstream} + a_2 R_{downstream}\right) + L \qquad (4)$$

with a_1=0 and a_2=0.4.

With these assumptions the critical number found is given by:

$$\frac{\theta}{W} = 0.0005 \qquad (5)$$

in which θ is the (laminar) momentum boundary layer and W the cavity width. This number is lower than the values found for side branches (≈0.1) or for cavities (0.01-0.025). Again, it is thought that part of the difference is due to the acoustic interaction and feedback from the boundary conditions, but the exact reasons are not known yet. From the critical boundary layer thickness hypothesis, it can already be concluded that corrugations with large plateaus would start to sing at higher velocities than the bellows type corrugated tubes. This also means that as the corrugations are in practice not symmetric, the installation direction is important. This is confirmed by the experiments. In Table 3 the measured onset velocities are given for the tested non-symmetric corrugations. The configurations with the largest edge radius upstream have a small onset velocity, due to the smaller boundary layer growth length available.

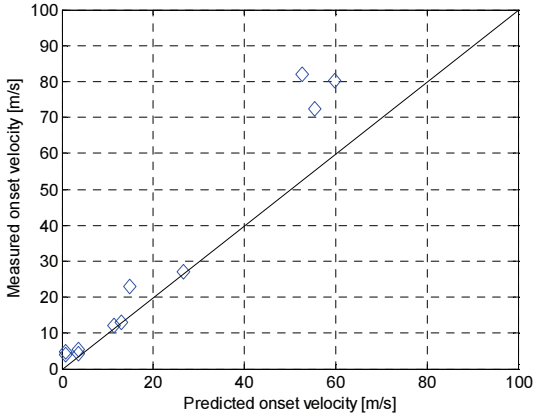

Figure 16: Measured onset velocity as a function of predicted onset velocity.

Table 3: Onset velocity (at atmospheric conditions) for non-symmetric corrugations. The A direction is the direction with the large edge radius upstream.

R1/R2 [mm/mm]	Uonset A [m/s]	Uonset B [m/s]
2/0.5	80	93
3/1	13	>96
4/0	12	>111

Furthermore, systems will start to whistle sooner at higher pressures, due to the effect of the density on the viscosity and the thinning boundary layer as a consequence. This effect is demonstrated in Figure 17 where the measured onset velocity is compared to the expected 1/density behaviour as a function of operating pressure.

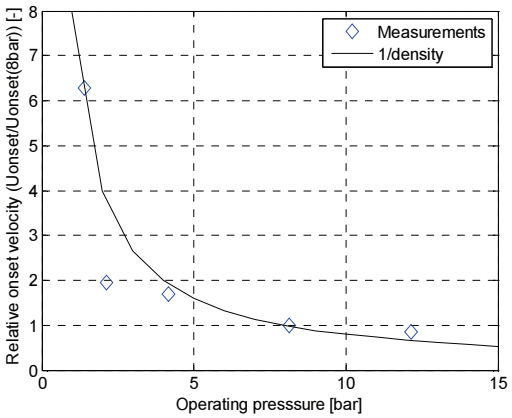

Figure 17: Measured onset velocity as a function of operation pressure and 1/density function.

CONCLUSIONS

Depending on the corrugation profile and the termination geometry, some corrugated tubes can generate a whistling tone with amplitudes up to several bars. These pulsations can lead to integrity issues in the up and downstream installation. The whistling behaviour has been experimentally investigated using 2" artificially corrugated tubes and 2" cable conduits. The tubes were found to generate tones at two distinct modes, including a higher mode with a Strouhal number around Sr=0.35 and a lower mode of Sr=0.1. The relevant length scale in the Strouhal number is not the pitch but a modified gap width defined as the length of the gap including the upstream edge but excluding the downstream edge radius. This length does not define the Strouhal number uniquely. The Strouhal number for a given geometry is further defined by the cavity volume or the ratio of the upstream edge radius to the gap width.

The amplitude of the pulsations scales with the acoustic pressure defined by the density, the speed of sound, and the gas velocity. After onset, the amplitude saturates to a constant relative amplitude. Maximum amplitudes in the order of 10% of the acoustic pressure are measured. This saturation amplitude scales with the corrugation volume. For a given corrugation geometry, this saturation amplitude is independent of pressure, tube length, or boundary condition.

The onset of the whistling behaviour is dependent on both the corrugated tube as well as the piping environment in which the tube is installed. The minimum onset velocity is determined by a critical momentum thickness of the boundary layer which grows at each corrugation. However, especially for smaller tubes, the boundary conditions, that is the reflection coefficient, determine the onset velocity significantly. Changes in the order of a factor of three have been measured due to changes in the downstream reflection coefficient. For long tubes, this dependency on the reflection coefficient has not been found.

ACKNOWLEDGMENTS

The work discussed in this paper was made possible by the contributions of BP, Bureau Veritas, ExxonMobil, Statoil and the UK Health and Safety Executive. Furthermore, use of the facilities and expertise at the Eindhoven University of Technology was very valuable in particular the help of Prof. A. Hirschberg, R. Tummers and J. Bastiaansen..

REFERENCES

[1] Swindell R., S.Belfroid, "Internal flow induced pulsation in flexible risers", OTC18895, to be presented OTC 2007
[2] Bruggeman J.C., "Flow induced pulsations in pipe systems", PhD thesis Eindhoven University of Technology 1987
[3] Peters M.C.A.M., Bokhorst E. van, "Flow-induced pulsations in pipe systems with closed side-branches, impact of flow direction", Proceedings of the Flow-induced vibration 2000 conference, Lucerne, Switzerland, June 2000.
[4] Hofmans G.C.J. , "Vortex sound in confined flows", PhD thesis Eindhoven University of Technology 1998
[5] Anthoine J., J-M Buchlin, A. Hirschberg," Theoretical modelling of the effect of the nozzle cavity volume on the resonance level in large solid rocket motors", 7th AiAA/CEAS Aeroacoustics conference (2001 Maastricht)
[6] Kooijman G, "Acoustic response of shear layers", PhD thesis Eindhoven University of technology 2007
[7] Oshkai P., D. Rockwell, M. Pollack, "Shallow cavity flow tones: transformation from large- to small-scale modes", JSV 280 (2005)
[8] Naudasher E., D. Rockwell, "Flow induced vibrations" (1994), 139

NOMENCLATURE

a	Open area ratio of multihole orifice [m]
a	Coefficient for laminar boundary layer growth [-]
a_1	Coefficient for upstream edge radius fraction boundary layer growth [-]
a_2	Coefficient for downstream edge radius fraction boundary layer growth [-]

c	Speed of sound [m/s]
f	Frequency [-]
f_0	First axial resonance mode of measurement system (measurement sections and corrugated tube).
k_v	Rossiter parameter [-]
L	Length scale [m]
L	Carcass plateau length [m]
M	Mach number [-]
M_{av}	Average of up- and downstream Mach number [-]
U	Mean velocity [m/s]
U_c	Convective velocity shear layer disturbance [m/s]
U_{avg}	Average of upstream and downstream velocity [m/s]
Sr	Strouhal number [-]
Re	Reynolds number [-]
R_1	Carcass edge radius (upstream edge in A direction)[m]
R_2	Carcass edge radius (downstream edge in A direction) [m]
R_{up}	Carcass upstream edge radius [m]
R_{down}	carcass downstream edge radius [m]
W	Carcass gap width excluding edge rounding [m]
x	Boundary layer growth length [m]
ν	Gas viscosity [m^2/s]
θ	Momentum boundary layer thickness [m]
ρ	Density [kg/m3]
ξ	Rossiter parameter [-]